Supporting Information for "Hydrological drivers of record-setting water level rise on Earth's largest lake system"

A.D. Gronewold[1,2], J. Bruxer[3], D. Durnford[4], J.P. Smith[5], A.H. Clites[1], F. Seglenieks[6], S.S. Qian[7], T.S. Hunter[1], V. Fortin[4]

Corresponding author: A.D. Gronewold, National Oceanic and Atmospheric Administration, Great Lakes Environmental Research Laboratory, 4840 South State Rd., Ann Arbor, MI 48108, USA. (drew.gronewold@noaa.gov)

[1]National Oceanic and Atmospheric Administration, Great Lakes Environmental Research Laboratory, Ann Arbor, Michigan, USA, 48108

[2]University of Michigan, Department of Civil and Environmental Engineering, Ann Arbor, Michigan USA, 48109

[3]Environment Canada, Great Lakes - St. Lawrence Regulation Office, Cornwall, Ontario, Canada K6H 6S2

[4]Canadian Meteorological Centre, Dorval, Quebec, Canada H9P 1J3

Contents of this file

1. Text S1 and S2

2. Figures S1 to S6

Additional Supporting Information (Files uploaded separately)

1. Model code

Introduction

This Supporting Information contains details of our Bayesian statistical model including model code, and a series of figures depicting the development and evolution of prior probability distributions, likelihood functions, posterior probability distributions, and bias for each model variable.

[5]University of Michigan, Cooperative Institute for Limnology and Ecosystems Research, Ann Arbor, Michigan USA, 48109

[6]Environment Canada, Canada Centre for Inland Waters, Burlington, ON

[7]University of Toledo, Department of Environmental Sciences, Toledo, Ohio USA, 43606

Text S1: Prior and posterior probability distributions and bias

A graphical representation of our approach to developing prior probability distributions for each model variable is included in figures S1 and S2. Similarly, a graphical representation of the evolution of posterior probability distributions, including prior probability distributions for each model variable, and likelihood functions derived from each data source, are included in figures S3 and S4. Finally, the inferred seasonal bias in each estimate is presented in figures S5 and S6. Likelihood functions for each "observation" were simulated using the model described in the following section. It is informative to note that prior probability distributions could have been developed in many different ways using different (or additional) data sources [including, for example, water budget estimates from the GRACE satellite missions, as described in *Wahr et al.*, 1998] and across different time periods; our approach here is intended to support assessment of drivers behind the recent water level surge, however we expect to use it as a stepping stone in future research that focuses on updating the long-term record of the water budget (i.e. dating back to the early 1900s) for all of the Great Lakes.

Text S2: Model code and implementation

BUGS and JAGS (we ultimately used JAGS for the results presented here) implement a Markov chain Monte Carlo (MCMC) procedure for simulating samples from the posterior probability distribution for selected model parameters [*Press*, 2003; *Bolstad*, 2004]. We ran simulations until each MCMC chain converged on the posterior, as indicated by a potential scale reduction factor $\hat{R}$ close to 1.0 [*Gelman et al.*, 2004]. The model code is included as a downloadable file from the on-line section of the Supporting Information for this manuscript.

References

Bolstad, W. M. (2004), *Introduction to Bayesian Statistics*, Wiley-Interscience, Hoboken, N.J.

Gelman, A. J., J. B. Carlin, H. S. Stern, and D. B. Rubin (2004), *Bayesian Data Analysis*, Chapman & Hall/CRC, Boca Raton, Florida.

Hunter, T. S., A. H. Clites, K. B. Campbell, and A. D. Gronewold (2015), Development and application of a monthly hydrometeorological database for the North American Great Lakes - Part I: precipitation, evaporation, runoff, and air temperature, *Journal of Great Lakes Research*, *41*(1), 65–77.

Press, S. J. (2003), *Subjective and Objective Bayesian Statistics: Principles, Models, and Applications*, Wiley-Interscience, Hoboken, NJ.

Wahr, J., M. Molenar, and F. Bryan (1998), Time variability of the Earth's gravity field: Hydrological and oceanic effects and their possible detection using GRACE, *Journal of Geophysical Research*, *103*(B12), 30,205–30,229.

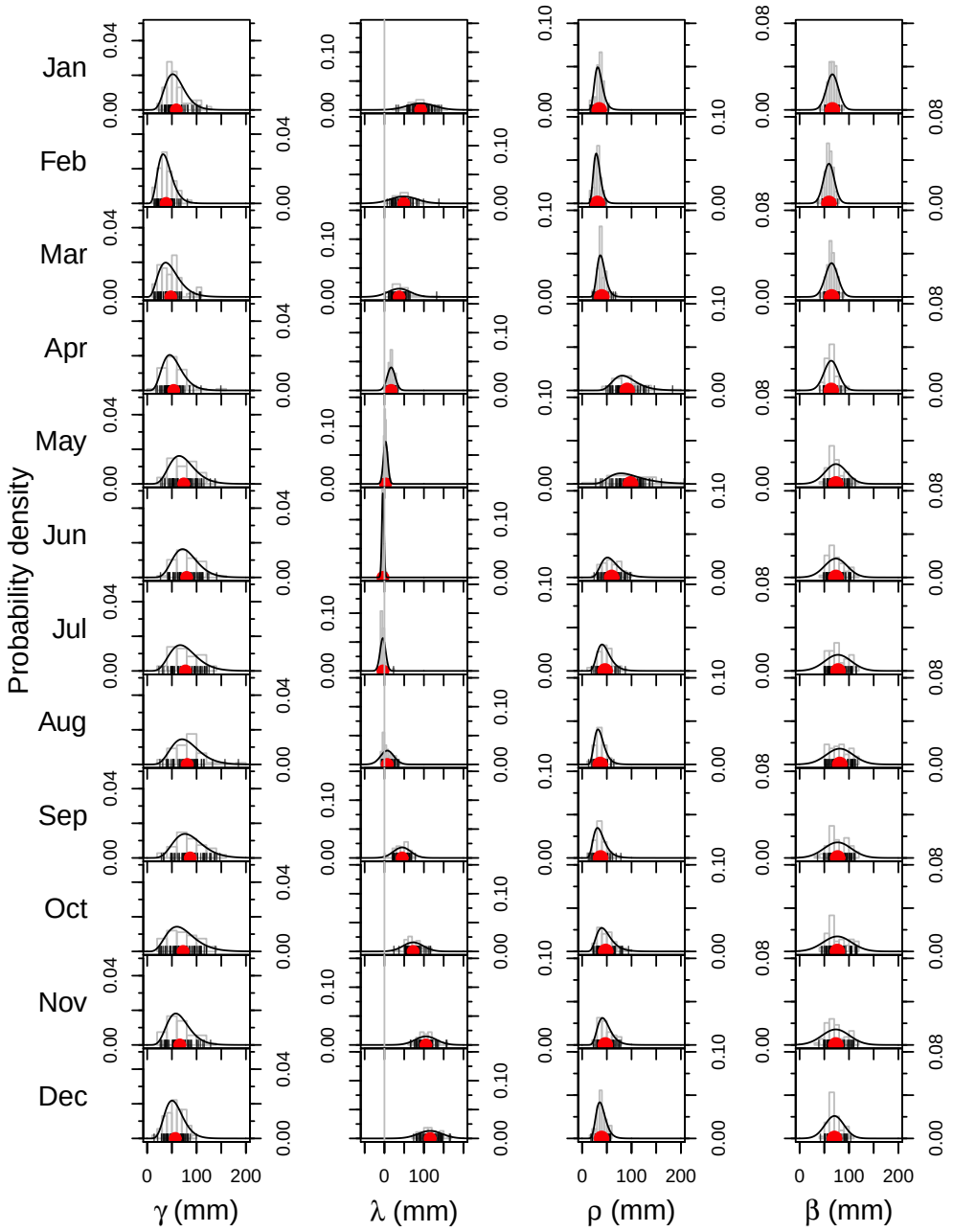

Figure S1. Development of prior probability distributions for Lake Superior water budget components. Vertical tick marks along x-axis and histograms are based on values from the historical record from 1950 to 2004 in the GLM-HMD [*Hunter et al.*, 2015]. Red dots represent the historical mean, and thin black curves represent the prior probability distributions described in the manuscript text.

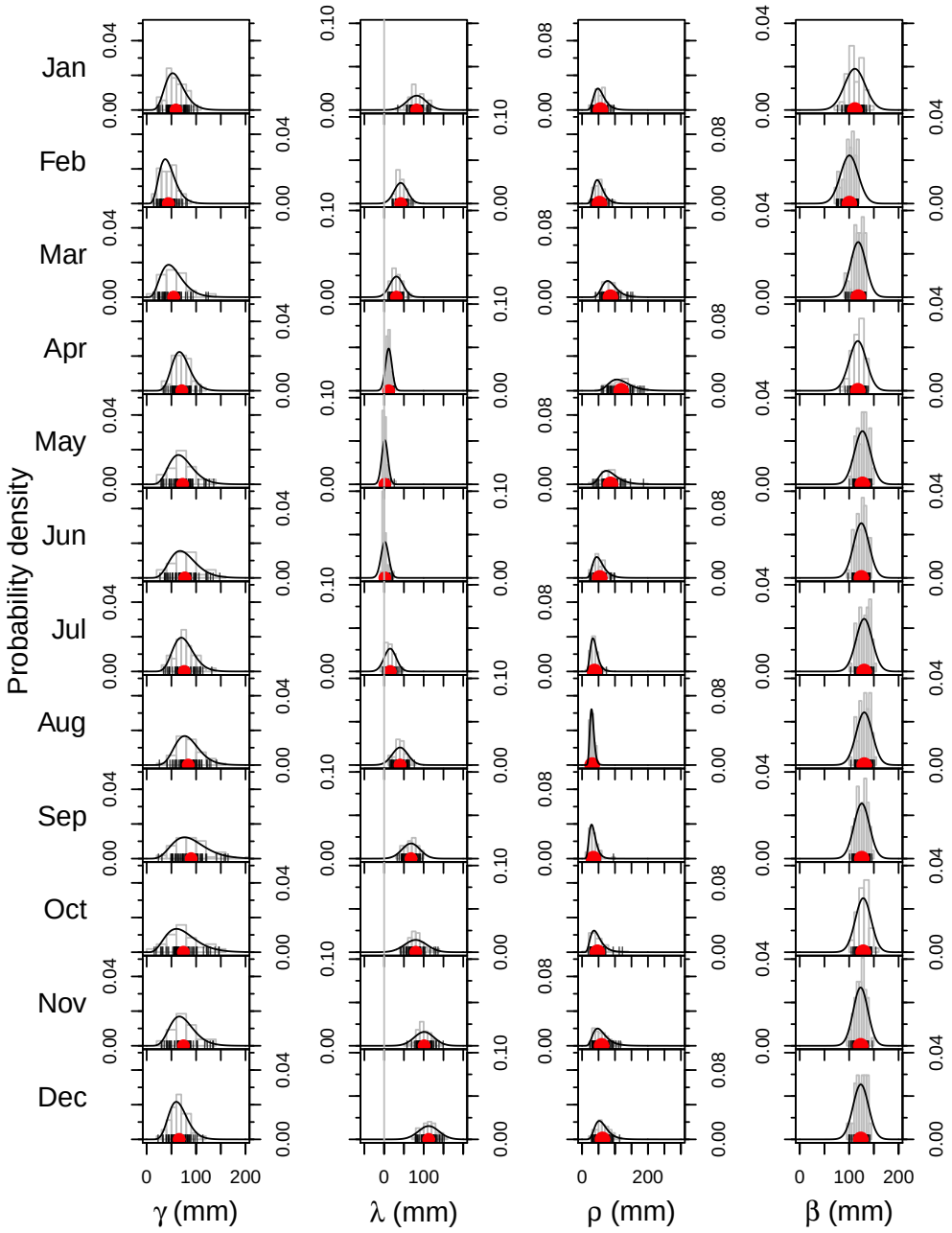

Figure S2. Development of prior probability distributions for Lake Michigan-Huron water budget components. Vertical tick marks along x-axis and histograms are based on values from the historical record from 1950 to 2004 in the GLM-HMD [*Hunter et al.*, 2015]. Red dots represent the historical mean, and thin black curves represent the prior probability distributions described in the manuscript text.

Figure S3. Evolution of posterior probability distributions for each water budget component on Lake Superior. In the three left-most columns, thin black curves represent prior probability distributions (from figure S1), blue curves represent likelihood functions from GEM models, red curves represent likelihood functions from GLM-HMD, and dark grey curves represent the posterior probability distribution for each monthly component (for 2013). In the right-most column, purple curves represent channel flow estimates from the international gaging stations, and green curves represent internationally-coordinated channel flow estimates.

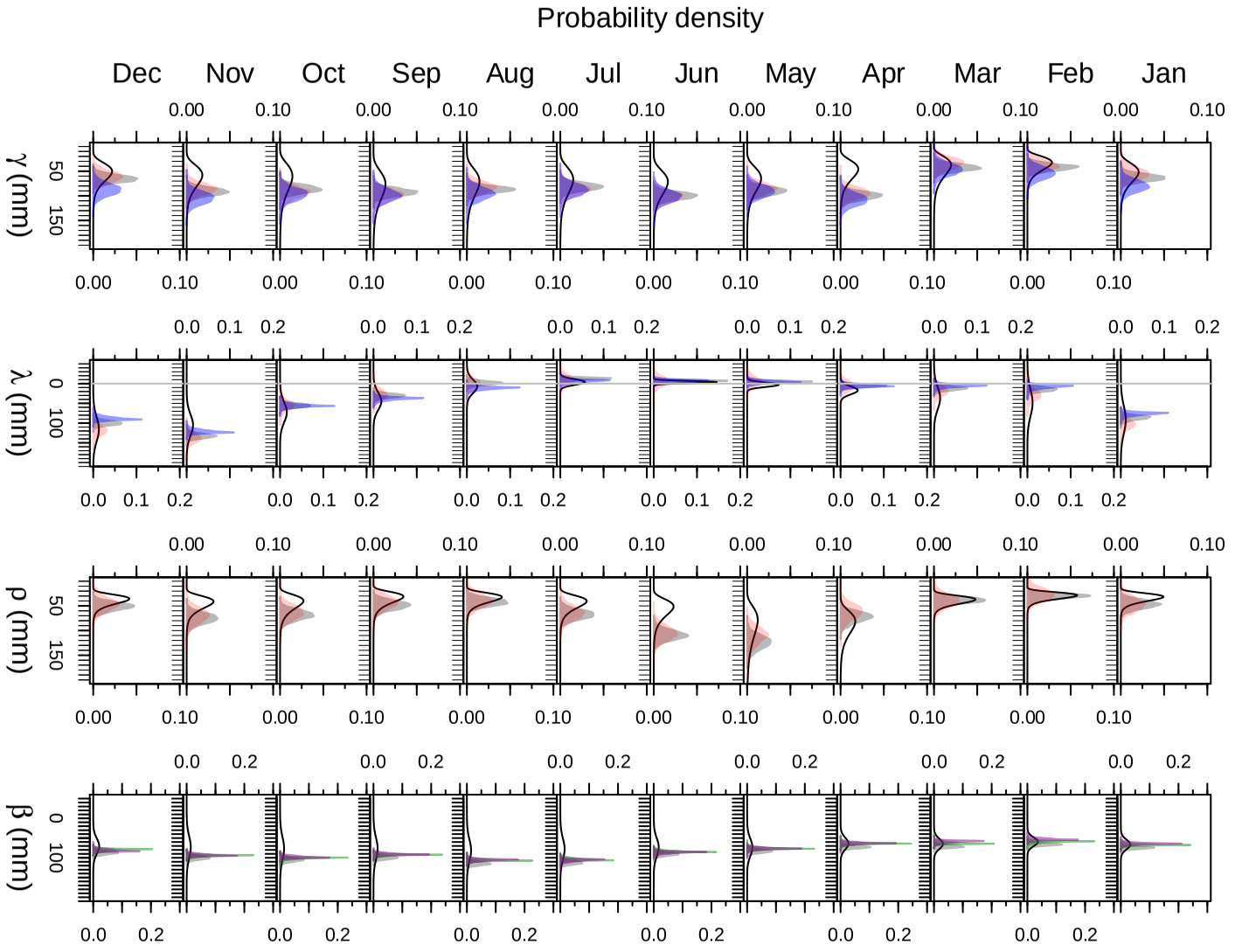
Probability density
Dec
Nov
Oct
Sep
Aug
Jul
Jun
May
Apr
Mar
Feb
Jan
γ (mm)
λ (mm)
ρ (mm)
β (mm)

Figure S4. Evolution of posterior probability distributions for each water budget component on Lake Michigan-Huron. In the three left-most columns, thin black curves represent prior probability distributions (from figure S2), blue curves represent likelihood functions from GEM models, red curves represent likelihood functions from GLM-HMD, and dark grey curves represent the posterior probability distribution for each monthly component (for 2013). In the right-most column, purple curves represent channel flow estimates from the international gaging stations, and green curves represent internationally-coordinated channel flow estimates.

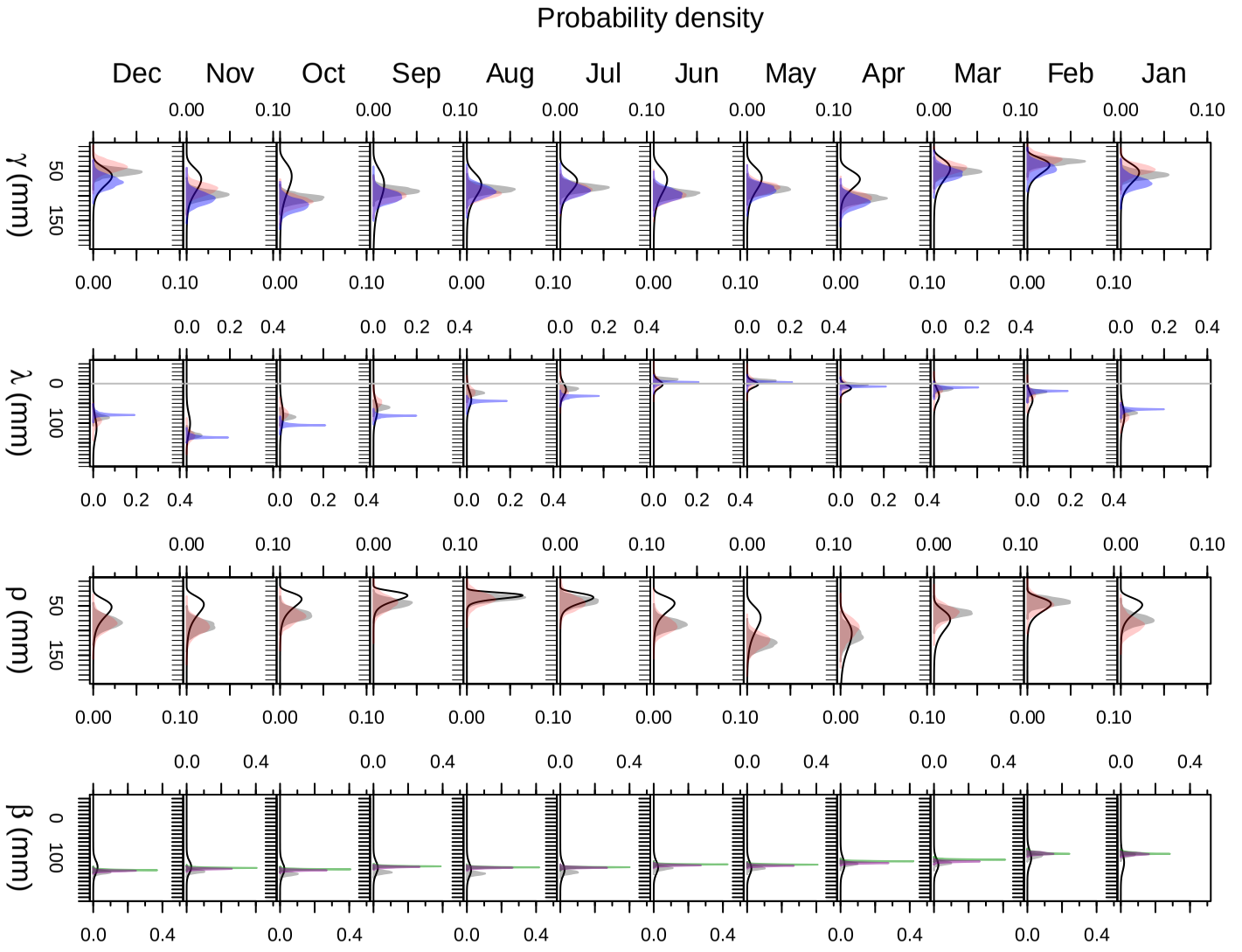
Probability density
Dec
Nov
Oct
Sep
Aug
Jul
Jun
May
Apr
Mar
Feb
Jan
γ (mm)
λ (mm)
ρ (mm)
β (mm)
0.00
0.10
0.0
0.2
0.4
50
150
0
100

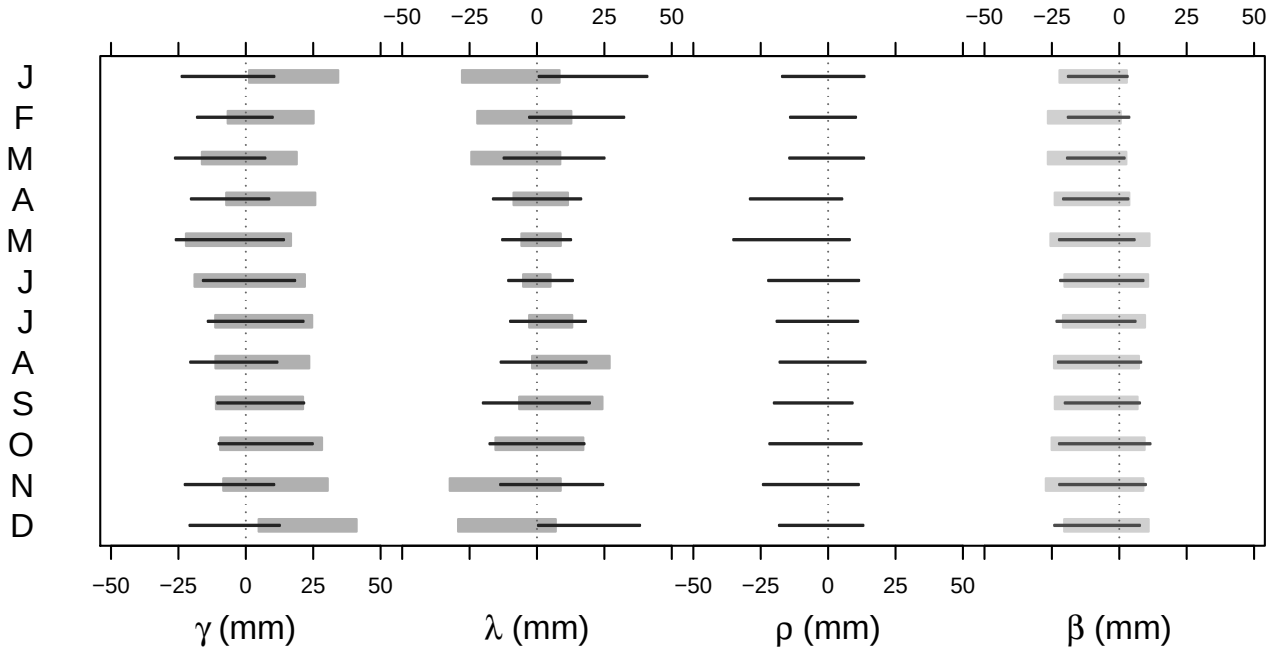

Figure S5. Seasonal bias (η) in Lake Superior monthly water budget estimates. For precipitation (γ), evaporation (λ), and runoff (ρ), thin black lines represent bias in GLM-HMD estimates and thick grey lines represent bias in GEM model estimates. For outflows (β), thin black lines represent bias in internationally-coordinated channel estimates and thick grey lines represent bias in the international gauging stations.

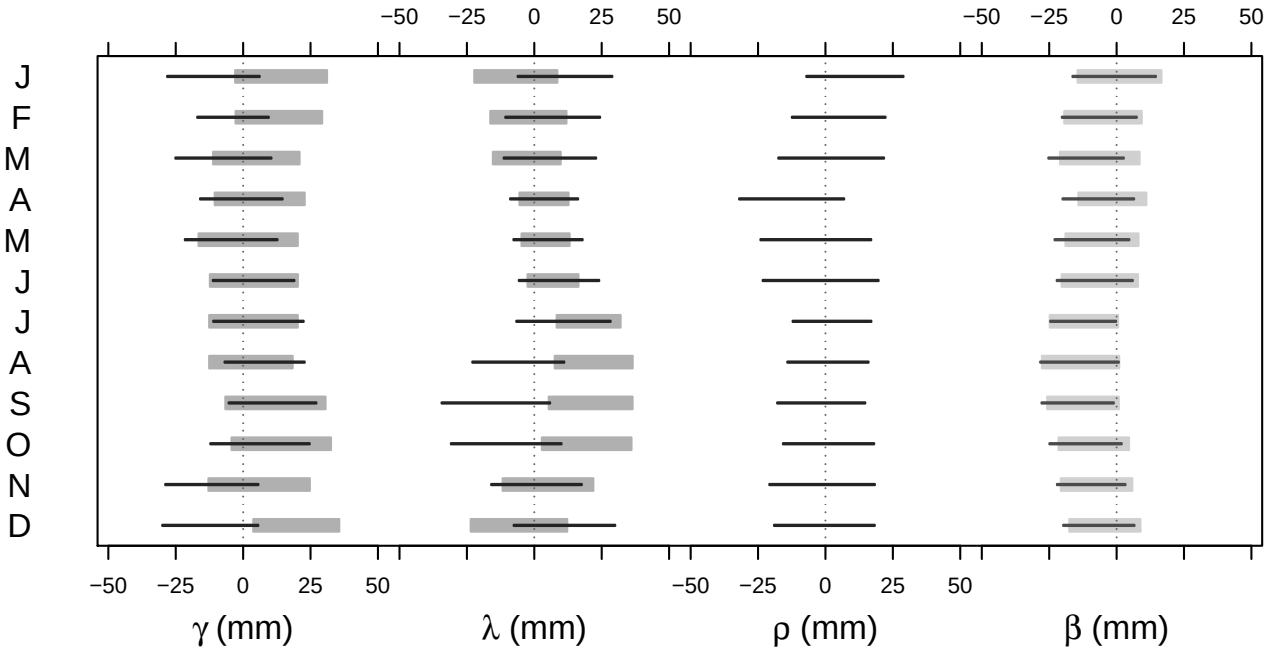

Figure S6. Seasonal bias (η) in Lake Michigan-Huron monthly water budget estimates. For precipitation (γ), evaporation (λ), and runoff (ρ), thin black lines represent bias in GLM-HMD estimates and thick grey lines represent bias in GEM model estimates. For outflows (β), thin black lines represent bias in internationally-coordinated channel estimates and thick grey lines represent bias in the international gauging stations.